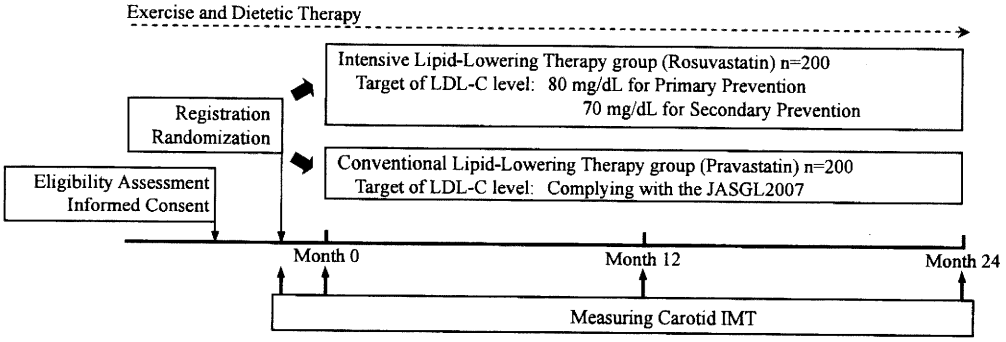

Fig. 1. Flow chart showing the study schedules.

IMT: intima-media thickness, JASGL2007: "Guidelines for Prevention of Atherosclerotic Cardiovascular Diseases (2007)" recommended by the Japan Atherosclerosis Society

Exclusion Criteria

(1) Patients that require lipid-lowering therapy other than with the study drug or specified lipid-lowering drugs (anion-exchange resin, probucol, and ethyl icosapentate (EPA)).

(2) Patients who have taken statins within 1 month of the start of the clinical trial.

(3) Patients suspected of having serious carotid artery stenosis (≥80%) or having serious calcification.

(4) Patients with familial hypercholesterolemia or secondary hypercholesterolemia.

(5) Patients with a fasting serum TG level ≥400 mg/dL.

(6) Patients with a history of sensitivity to statins.

(7) Patients with uncontrolled hypertension.

(8) Patients with Type I diabetes or uncontrolled Type II diabetes.

(9) Patients who have experienced myocardial infarction or a cerebral stroke within 3 months or patients with serious heart failure (New York Heart Association class III to IV).

(10) Patients with active hepatic disease.

(11) Patients with renal disorder [serum creatinine (Cr) level ≥2.0 mg/dL or creatinine clearance (Ccr) <30 mL/min/1.73 m^2].

(12) Patients with creatinine kinase (CK) level >500 IU/L.

(13) Patients currently being treated with cyclosporine.

(14) Patients that are pregnant or potentially pregnant, patients breast-feeding, or patients aiming to become pregnant during the clinical trial.

(15) Patients with or suspected of having a malignant tumor, or patients with a history of malignant tumors except those in whom recurrences have not been confirmed by routine observation after treatment.

(16) Patients with hypothyroidism, hereditary muscular diseases (muscular dystrophy, etc.) or a familial history of these diseases. Patients with a history of drug-related muscular disorders.

(17) Patients with a history of drug abuse or alcoholism.

(18) Patients who are ineligible in the opinion of the investigator.

In advance of the initiation of the clinical trial, the protocol was approved by the appropriate institutional review board or an independent ethics committee at each site.

Medications and Treatment Period

The eligible patients will be randomly assigned to receive either intensive lipid-lowering treatment with rosuvastatin or conventional lipid-lowering treatment with pravastatin under the instructions of the registration center. For equalization between the arms, patients will be dynamically assigned based on i) maximum IMT, ii) serum LDL-C, iii) anamnestic diabetes (including abnormal glucose tolerance), and iv) institution. The patients will be administered rosuvastatin for 24 months at an initial dose of 5mg once daily or pravastatin at 10 mg once daily. If the initial treatment fails to reduce the target LDL-C level, the dose can be increased to 10 mg/day for rosuvastatin or 20 mg/day for pravastatin (**Fig. 1**). Furthermore, the investigator-in-charge is allowed to administer combination therapy with anion-exchange resin, probucol or EPA, if the increased dose of each test drug fails to reduce the target LDL-C level.

Sample Size

In the protocol, the assumptions used for power calculations require a sample size of 173 patients to provide 90% power (assuming a SD of 1.0%) and an alpha level of 0.05% for a two-sided test. It is there-

Table 1. Items and schedule

Schedule	Registration	Treatment period								
Items	VISIT 1 Month −1~0	VISIT 2 Month 0	VISIT 3 Month 1	VISIT 4 Month 2	VISIT 5 Month 4	VISIT 6 Month 6	VISIT 7 Month 12	VISIT 8 Month 18	VISIT 9 Momth 24 (Completion)	At discontinuation
Patients characteristics	○									
Blood pressure (Systolic, Diastolic)		○					○		○	○
Carotid IMT measurement	○	○					○		○	○
Blood chemistry										
Other parameters except HbA1c		○	○		○	○	○		○	○
HbA1c		○					○		○	○
Serum lipids		○	○	○	○	○	○	○	○	○
Adverse events		○	○	○	○	○	○	○	○	○

Carotid IMT measurement: max-IMT, maximal carotid IMT, maximal carotid sinus IMT and maximal internal carotid artery IMT will be measured with a B-mode ultrasound at each study site. Mean-IMT will be determined in the laboratory. Carotid IMT measurements at VISIT 1 and VISTI 2 are for considering eligibility at each study site and obtaining baseline values for treatment in the laboratory, respectively.
Blood chemistry tests: aspartate aminotransferase, alanine aminotransferase, γ-glutamyl transpeptidase, blood urea nitrogen, creatinine, creatine kinase and HbA1c.
Serum lipids: total cholesterol, low-density lipoprotein cholesterol, high-density lipoprotein cholesterol and triglycerides
IMT: intima-media thickness, HbA1c: glycosylated hemoglobin

fore determined that the enrollment of 200 patients per treatment will provide an adequate number of patients considering possible discontinuations and dropouts.

Observation Items and Schedule

The observation items and schedule are shown in **Table 1**.

Efficacy Evaluation

Primary Endpoint

The percent changes from baseline in mean-IMT at the end of 24 months. The mean IMT is the average of the maximum IMTs before and after treatment.

Secondary Endpoint

The following 12 endpoints will be evaluated.

(1) Time to percent change in mean-IMT.

(2) Time to percent change in max-IMT of the distal wall of the common carotid artery (IMT-Cmax-distal wall).

(3) Time to percent change in IMT-Cmax of the common carotid artery, IMT-Bmax of the carotid sinus, and IMT-Imax of the internal carotid artery.

(4) Percentage of cases in which mean-IMT decreased at the end of 12 months and 24 months.

(5) Time to percent change in the LDL-C/HDL-C ratio.

(6) Percentage of cases in which the LDL-C/HDL-C ratio was ≤1.5 at the end of 12 months and 24 months.

(7) Percentage of cases in which the LDL-C/HDL-C ratio was ≤2.0 at the end of 12 months and 24 months.

(8) Correlation between the LDL-C/HDL-C ratio and max-IMT.

(9) Correlation between the LDL-C/HDL-C ratio and mean-IMT.

(10) Time to percent change of serum lipids (LDL-C, HDL-C, and TG), glycosylated hemoglobin (HbA1c), systolic blood pressure, and diastolic blood pressure.

(11) JASGL2007 achievement ratio according to the management target level of LDL-C.

(12) Cumulative incidence and content of cardiovascular and cerebrovascular events.

Cardiac events: myocardial infarction, angina pectoris, congestive heart failure, and coronary artery bypass graft

Cerebrovascular events: cerebral hemorrhage, cerebral infarction, subarachnoid hemorrhage, and transient ischemic attack

Safety Evaluation

Details and incidence of adverse events.

Analysis Population

Full Analysis Set (FAS): All allocated patients

except those who did not receive the test drug at all during the treatment period, patients whose IMTs were not measured at all during the observation and treatment periods, or patients for which the results of the of efficacy evaluation were insufficient for analysis.

Per Protocol Set (PPS): The FAS population except patients who did not meet the inclusion and exclusion criteria, patients whose compliance with the therapy was less than 75%, patients who were administered a prohibited drug in the study protocol, or patients who had insufficient IMT data at the start and completion of the study.

Safety Population (SP): All allocated patients except those who did not receive the test drug at all during the treatment period, or patients who had no observation record after allocation of the study.

Statistical Analysis

Evaluation of Efficacy: In the FAS and PPS, the mean-IMT value at the start of the study will be used as a baseline for calculating the percent change in Month 24, as well as the two-sided 95% confidence interval. The two-sided level of significance will be set at $p<0.05$.

Safety Evaluation: In the SP, the incidence of each adverse event will be calculated for each group. The basal analytical amount and incidence of abnormality for each parameter of laboratory tests will be calculated for each group.

Compliance with the Ethical Principles in Clinical Studies and the Declaration of Helsinki

The study is to be conducted in accordance with the Ethical Principles in Clinical Studies published by the Ministry of Health, Labor and Welfare of Japan and the ethical principles originating in the Declaration of Helsinki.

Privacy Protection of Study Patients

The study is to be conducted in compliance with the following points to protect the privacy of the study patients. The confidentiality of each patient's information should be strictly maintained.

1. Attention to the treatment of medical records related to the study (including IMT image information, Informed Consent Form, etc.
2. Some patient information should not be inputed into the support system of the clinical study.
3. Patient anonymity must be maintained when the results of the study are published.
4. Data obtained from the study should not be used for any other purpose except the study objectives.
5. In the case where clinical samples are measured in other laboratories, the samples should be treated in accordance with the ethical guidelines of the clinical trial (assumed name, storage and disposal of the test drugs, limitation of access to data, etc).

Study Organization

Principle Investigator

Ryuji Nohara, Division of Cardiology, Kitano Hospital, Tazuke Kofukai Medical Research Institute, Osaka, Japan

Steering Committee

Ryuji Nohara, Division of Cardiology, Kitano Hospital, Tazuke Kofukai Medical Research Institute, Osaka, Japan

Ichiro Sakuma, Hokko Memorial Clinic Caress Sapporo, Sapporo, Japan

Masahiko Kurabayashi, Department of Medicine and Biological Science, Gunma University Graduate School of Medicine, Maebashi, Japan

Ryuzo Kawamori, Department of Medicine, Juntendo University School of Medicine, Tokyo, Japan

Hiroyuki Daida, Department of Cardiovascular Medicine, Juntendo University School of Medicine, Tokyo, Japan

Tsutomu Yamazaki, Department of Clinical Epidemiology & Systems, Graduate School of Medicine, University of Tokyo, Tokyo, Japan

Masayuki Yoshida, Life Science and Bioethics Research Center, Graduate School of Medicine, Tokyo Medical and Dental University, Tokyo, Japan

Mitsumasa Hata, Department of Cardiovascular Surgery, Nihon University School of Medicine, Tokyo, Japan

Izuru Masuda, Department of Internal Medicine, Higashiyama Takeda Hospital, Kyoto, Japan

Kohei Kaku, Division of Diabetes and Endocrinology, Department of Medicine, Kawasaki Medical School, Kurashiki, Japan

Hiroyoshi Yokoi, Department of Cardiology, Kokura Memorial Hospital, Kitakyushu, Japan

Data and Safety Evaluation Committee

Tadatoshi Takayama, Department of Digestive Surgery, Nihon University School of Medicine, Japan

Junji Kishimoto, Department of Digital Organ, Digital Medicine Initiative, Kyushu University, Fukuoka, Japan

Person in Charge of the Core Laboratory for IMT Evaluations

Ryuzo Kawamori, Department of Medicine, Juntendo University School of Medicine, Tokyo, Japan

Statistician
Junji Kishimoto, Department of Digital Organ, Digital Medicine Initiative, Kyushu University, Fukuoka, Japan

Discussion

Recent randomized clinical trials have confirmed that intensive LDL-C lowering therapy reduces the incidence of CAD in both primary and secondary prevention, and a meta-analysis of major statin trials revealed that the greater the reduction in LDL-C, the greater the reduction in risk for CAD[15, 16]. However, questions remain regarding the specific level of LDL-C needed to achieve the regression of carotid IMT.

In the METEOR trial, LDL-C was decreased to 78 mg/dL and carotid IMT was decreased by 0.0014 mm/year in the rosuvastatin (40 mg/day) group whereas the group given a placebo showed a progression of IMT after 2 years of follow-up[14]. However, the effect of rosuvastatin on IMT in Japanese patients has not yet been investigated. The present study was designed to evaluate this effect.

Carotid IMT is a highly reproducible and reliable measure[17]. A cardiovascular Health Study showed that asymptomatic persons without clinical symptoms or signs of cardiovascular disease 65 years of age or older had a higher risk of myocardial infarction or stroke, when their maximum IMT was 1.18 mm or more in the common and internal carotid artery[18]. In a nested case-control study in subjects selected from participants in the Rotterdam study, IMT of the common carotid was significantly increased in subjects with myocardial infarction compared to controls (1.17 mm vs 1.02 mm, $p<0.05$)[19]. It has also been reported that increased carotid IMT relates to an increase in the risk of cardiovascular disease even in asymptomatic individuals including young populations[20, 21], and carotid IMT is useful as a surrogate marker for cardiovascular events in intervention studies[22]. Particularly in studies of statins, carotid IMT has proved a highly reliable surrogate marker; a decrease in carotid IMT correlates well with a decrease in the risk of cardiovascular events[13]. B-mode ultrasound is widely used in clinical practice to measure carotid IMT non-invasively. However, this technique is likely to cause inter-institutional variation in measurements due to differences in the device used, and non-uniformity of the protocol involved etc. In the present study, the endpoint, changes of carotid IMT, will be evaluated in the IMT Core Laboratory in a blinded manner, to adequately maintain objectivity, scientific credibility, and ethics. This study will be conducted as a multi-center, prospective, randomized, open-label, evaluator-blinded, parallel-group, comparative study that incorporates a safety evaluation committee and statistical experts, to evaluate the effect of rosuvastatin on carotid IMT.

In a high-resolution magnetic resonance imaging trial to evaluate the effect of rosuvastatin therapy on the morphology and composition of carotid plaques in moderately hypercholesterolemic patients (the ORION trial), treatment with rosuvastatin at 5 mg/day and 40 mg/day for 2 years decreased LDL-C levels from 153.6 mg/dL to 95.0 mg/dL and from 145.0 mg/dL to 57.7 mg/dL, respectively, leading to a 41.4% decrease from baseline in the lipid-rich necrotic core[23]. In the METEOR trial, significant suppression of carotid IMT was observed when the LDL-C level was decreased to 78 mg/dL by treatment with rosuvastatin at 40 mg/day for 2 years[14]. Also in the ASTEROID trial, a significant decrease in coronary plaque volume was observed when the LDL-C level was decreased to 60.8 mg/dL by intensive treatment with rosuvastatin at 40 mg/day for 2 years[9].

Based on the results of these studies, we decided to compare changes in carotid IMT between an intensive treatment group and a conventional treatment group: in the former group, lipid management will be conducted with reference to the target LDL-C level specified by NCEP ATP Ⅲ with the objective of decreasing the incidence of coronary artery disease; and in the latter group, the target level specified in the JASGL2007 will be adopted. If carotid IMT regression is not evident in the conventional group but is observed in the intensive treatment group, this study will provide new insight and guidance for the target level of LDL-C in order to induce regression of atherosclerosis in the Japanese population.

Acknowledgments

A Japan Heart Foundation Research Grant will support this study registered to the University hospital Medical Information Network (UMIN) as ID UMIN000001174.

References

1) Scandinavian Simvastatin Survival Study Group: Randomised trial of cholesterol lowering in 4,444 patients with coronary heart disease: The Scandinavian Simvastatin Survival Study (4S). Lancet, 1994; 344: 1383-1389
2) Sacks FM, Pfeffer MA, Moye LA, Rouleau JL, Rutherford JD, Cole TG, Brown L, Warnica JW, Arnold JM, Wun CC, Davis BR, Braunwald E: The effect of pravastatin on coronary events after myocardial infarction in patients with average cholesterol levels. N Engl J Med, 1996; 335:

1001-1009
3) Keech A, Colquhoun D, Best J, Kirby A, Simes RJ, Hunt D, Hague W, Beller E, Arulchelvam M, Baker J, Tonkin A; LIPID Study Group: Secondary prevention of cardiovascular events with long-term pravastatin in patients with diabetes or impaired fasting glucose: results from the LIPID trial. Diabetes Care, 2003; 26: 2713-2721
4) Saeki T, Sakuma N, Hayakawa K, Itou K, Wakami K, Tamai N, Kimura G: Low incidence of cardiac events in statin-administered patients in CAG study. J Atheroscler Thromb, 2009; Jun 25
5) Nagashima H, Kasanuki H: The status of lipid management in 1,836 patients with coronary artery disease: a multicenter survey to evaluate the percentage of Japanese coronary artery disease patients achieving the target low-density lipoprotein cholesterol level specified by the Japan Atherosclerosis Society. J Atheroscler Thromb, 2005; 12: 338-342
6) Ito H, Ouchi Y, Ohashi Y, Saito Y, Ishikawa T, Nakamura H, Orimo H: A comparison of low versus standard dose pravastatin therapy for the prevention of cardiovascular events in the elderly: the pravastatin anti-atherosclerosis trial in the elderly (PATE). J Atheroscler Thromb, 2001; 8: 33-44. Erratum in: J Atheroscler Thromb, 2001; 8: following 100
7) von Birgelen C, Hartmann M, Mintz GS, Baumgart D, Schmermund A, Erbel R: Relation between progression and regression of atherosclerotic left main coronary artery disease and serum cholesterol levels as assessed with serial long-term (>or=12 months) follow-up intravascular ultrasound. Circulation, 2003; 108: 2757-2762
8) Okazaki S, Yokoyama T, Miyauchi K, Shimada K, Kurata T, Sato H, Daida H: Early statin treatment in patients with acute coronary syndrome: demonstration of the beneficial effect on atherosclerotic lesions by serial volumetric intravascular ultrasound analysis during half a year after coronary event: the ESTABLISH Study. Circulation, 2004; 110: 1061-1068
9) Nissen SE, Nicholls SJ, Sipahi I, Libby P, Raichlen JS, Ballantyne CM, Davignon J, Erbel R, Fruchart JC, Tardif JC, Schoenhagen P, Crowe T, Cain V, Wolski K, Goormastic M, Tuzcu EM; ASTEROID Investigators: Effect of very high-intensity statin therapy on regression of coronary atherosclerosis: the ASTEROID trial. JAMA, 2006; 295: 1556-1565
10) Nicholls SJ, Tuzcu EM, Sipahi I, Grasso AW, Schoenhagen P, Hu T, Wolski K, Crowe T, Desai MY, Hazen SL, Kapadia SR, Nissen SE: Statins, high-density lipoprotein cholesterol, and regression of coronary atherosclerosis. JAMA, 2007; 297: 499-508
11) Takayama T, Hiro T, Yamagishi M, Daida H, Saito S, Yamaguchi T, Matsuzaki M: Rationale and design for a study using intravascular ultrasound to evaluate effects of rosuvastatin on coronary artery atheroma in Japanese subjects: COSMOS study (Coronary Atherosclerosis Study Measuring Effects of Rosuvastatin Using Intravascular Ultrasound in Japanese Subjects). Circ J, 2007; 71: 271-275
12) Miyauchi K, Kimura T, Morimoto T, Nakagawa Y, Yamagishi M, Ozaki Y, Hiro T, Daida H, Matsuzaki M: Japan assessment of pitavastatin and atorvastatin in acute coronary syndrome (JAPAN-ACS): rationale and design. Circ J, 2006; 70: 1624-1628
13) Espeland MA, O'leary DH, Terry JG, Morgan T, Evans G, Mudra H: Carotid intimal-media thickness as a surrogate for cardiovascular disease events in trials of HMG-CoA reductase inhibitors. Curr Control Trials Cardiovasc Med, 2005; 6: 3
14) Crouse JR 3rd, Raichlen JS, Riley WA, Evans GW, Palmer MK, O'Leary DH, Grobbee DE, Bots ML; METEOR Study Group: Effect of rosuvastatin on progression of carotid intima-media thickness in low-risk individuals with subclinical atherosclerosis: the METEOR Trial. JAMA, 2007; 297: 1344-1353
15) LaRosa JC, Grundy SM, Waters DD, Shear C, Barter P, Fruchart JC, Gotto AM, Phil D, Greten H, Kastelein JJ, Shepherd J, Wenger NK; Treating to New Targets (TNT) Investigators: Intensive lipid lowering with atorvastatin in patients with stable coronary disease. N Engl J Med, 2005; 352: 1425-1435
16) Ridker PM, Danielson E, Fonseca FA, Genest J, Gotto AM Jr, Kastelein JJ, Koening W, Libby P, Lorenzatti AJ, MacFadyen JG, Nordestgaard BG, Shepherd J, Willerson JT, Glynn RJ; JUPITER Study Group: Rosuvastatin to prevent vascular events in men and women with elevated c-reactive protein. N Engl J Med, 2008; 359: 2195-2207
17) Bots ML, Evans GW, Riley WA, Grobbee DE: Carotid intima-media thickness measurements in intervention studies: design options, progression rates, and sample size considerations: a point of view. Stroke, 2003; 34: 2985-2994
18) O'Leary DH, Polak JF, Kronmal RA, Manolio TA, Burke GL, Wolfson SK Jr: Carotid-artery intima and media thickness as a risk factor for myocardial infarction and stroke in older adults. Cardiovascular Health Study Collaborative Research Group. N Engl J Med, 1999; 340: 14-22
19) del Sol AI, Moons KG, Hollander M, Hofman A, Koudstaal PJ, Grobbee DE, Breteler MM, Witteman JC, Bots ML: Is carotid intima-media thickness useful in cardiovascular disease risk assessment? The Rotterdam Study. Stroke, 2001; 32: 1532-1538
20) Davis PH, Dawson JD, Riley WA, Lauer RM: Carotid intimal-medial thickness is related to cardiovascular risk factors measured from childhood through middle age: the Muscatine Study. Circulation, 2001; 104: 2815-2819
21) Oren A, Vos LE, Uiterwaal CS, Grobbee DE, Bots ML: Cardiovascular risk factors and increased carotid intima-media thickness in healthy young adults: the Atherosclerosis Risk in Young Adults (ARYA) Study. Arch Intern Med, 2003; 163: 1787-1792
22) Bots ML: Carotid intima-media thickness as a surrogate marker for cardiovascular disease in intervention studies. Curr Med Res Opin, 2006; 22: 2181-2190
23) Underhill HR, Yuan C, Zhao XQ, Kraiss LW, Parker DL, Saam T, Chu B, Takaya N, Liu F, Polissar NL, Neradilek B, Raichlen JS, Cain VA, Waterton JC, Hamar W, Hatsukami TS: Effect of rosuvastatin therapy on carotid plaque morphology and composition in moderately hypercholesterolemic patients: A high-resolution magnetic resonance imaging trial. Am Heart J, 2008; 155: 584e1-584e8

Case Report

AV Nodal Reentrant Tachycardia in a Patient with Persistent Left Superior Vena Cava: Distinction between AV Nodal Versus Atrial Reentry

Terunobu Fukuda MD, Tetsuya Haruna MD, Hidehiro Ito MD, Kenichi Sasaki MD, Tomomi Abe MD, Eisaku Nakane MD, Shouichi Miyamoto MD, Kyoukun Uehara MD, Muneo Ooba MD, Kouji Ueyama MD, Moriaki Inoko MD, Ryuji Nohara MD

Department of Cardiology, Kitano Hospital Medical Research Institute

A 75-year-old male presented with palpitation on exertion. He suffered from frequent tachycardia attacks. His 12-leads electrocardiogram showed irregular cycle lengths (400–550 ms) of tachycardia with occasional 2:1 atrioventricular conduction (thus AV reentry was excluded). He had a complex anatomy of persistent left superior vena cava (PLSVC)/enlarged coronary sinus (CS). The activation map in a 3-dimensional CARTO system (Biosense-Webster, USA) was merged with the multi-detector computed tomography image and revealed that the tachycardia spread centrifugally from the junction between the PLSVC and enlarged CS. However, delivery of radio frequency (RF) energy to the earliest atrial activation site did not affect the tachycardia. Finally, the tachycardia was diagnosed as a fast/slow type atrioventricular nodal reentrant tachycardia (AVNRT) because the tachycardia was cured only after the anterograde/retrograde AV conduction was disturbed by the application of RF energy to the posteroseptal perimitral area, possibly due to the injury to the AV node. (J Arrhythmia 2010; 26: 134–139)

Key words: Persistent left superior vena cave, Atrial tachycardia, Enlarged coronary sinus, Radiofrequency catheter ablation

Introduction

During normal development, the left superior vena cava transforms into the Marshall vein/ligament and rarely remains intact as the persistent left superior vena cava (PLSVC), and connects to the coronary sinus (CS).[1–4] Recently, the Marshall vein/ligaments have been reported to be associated with atrial arrhythmogenesis.[3–8] On the other hand, it has been reported that the enlarged CS from the PLSVC could displace the compact atrioventricular (AV) node and the His-bundle.[9] Therefore, much attention should be paid to avoid injury of the compact AV node and His-bundle during application of radio-frequency (RF) energy.[9]

We experienced a type of fast/slow atrioventricular nodal reentrant tachycardia (AVNRT), which was difficult to differentiate from an atrial reentrant tachycardia in a patient with the PLSVC and enlarged CS. The AVNRT was distinguished from

Received 18, February, 2009: accepted 15, February, 2010.
Address for correspondence: Tetsuya Haruna, MD, PhD, Department of Heart Center, Kitano Hospital Medical Research Institute, 2-4-20 Ohgimachi Kita-ku, Osaka 530-8480, Japan. Phone: 81-6-6312-1221 Fax: 81-6-6312-8867 Mail address: haruna@kitano-hp.or.jp

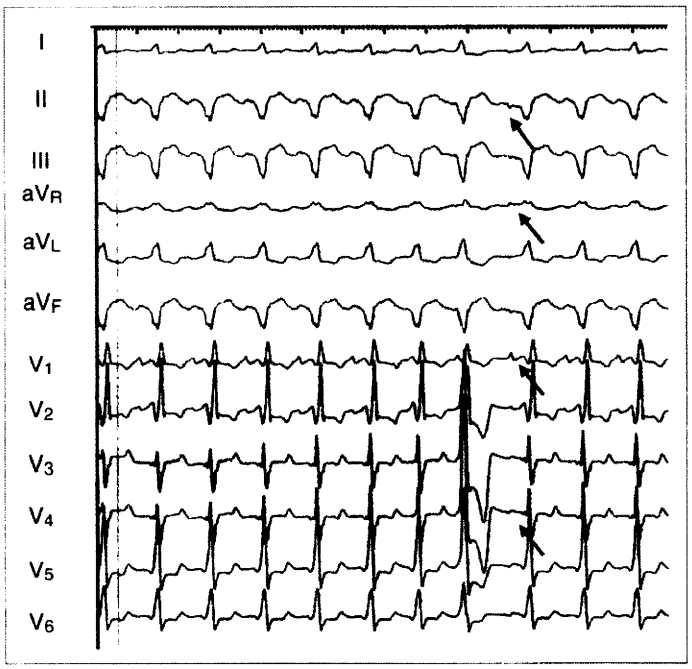

Figure 1 A 12-lead electrocardiogram of the tachycardia at 25 mm/s paper speed.
Arrows indicate the P-wave of the tachycardia.

the atrial reentrant tachycardia as follows; the tachycardia elimination was made possible only after the (partial) damage to the anterograde/retrograde AV nodal pathways was obtained by the application of RF energy to the AV junctional area. A new 3-dimensional electroanatomical mapping system (CARTO Merge, Boston, USA) was very helpful in the RF catheter ablation procedure.

Case Report

A 75-year-old man complained of palpitation and faintness on exertion. He underwent bypass graft surgery for coarctation of the descending aorta and right atrium (RA) isthmus catheter ablation for common atrial flutter at the age of 65 and 68 years, respectively. He had a 6-year-history of another tachycardia, and his 12-lead electrocardiogram (ECG) showed an irregular cycle length of the supraventricular tachycardia with a 1:1 or infrequently a 2:1 AV ratio and right bundle branch block. Axis in the P-wave morphology was biphasic (+/−) on I, II, III, aVF, and V1 leads (**Figure 1**). Chest X-ray showed an enlarged cardiac silhouette. Contrast computed tomography of the thorax revealed that the PLSVC was draining into the enlarged CS and the RA.

Although the supraventricular tachycardia was partially controlled with propafenone (300 mg/day), pirmenol (100 mg/day), and carvedilol (5 mg/day), he still suffered from palpitation and faintness on exertion. In addition, the QRS duration increased gradually. Echocardiography showed that the left ventricle ejection fraction (LVEF) was reduced to 35% as compared to that in the previous study (61%). The patient wished to discontinue all anti-arrhythmic agents and undergo RF catheter ablation. We obtained written informed consent from the patient. Electrophysiological study and catheter ablation were performed 3 days after discontinuation of all anti-arrhythmic agents. First, the anatomy of the enlarged CS and the RA was visualized by both RA angiography and contrast infusion into the PLSVC (**Figures 2A** and **2B**). The junction between the PLSVC and the enlarged CS, however, could not be clearly identified. A decapolar 7-Fr electrode catheter (Nihon Koden, Japan) was advanced into the CS via the right internal jugular vein for recording and pacing at both the RA and the CS. A 7-Fr Halo catheter (SJM, Irvin, USA) was introduced into the RA via the right femoral vein and positioned around the Tricuspid Annulus (TA). A 4-mm tip of a Navistar catheter (Biosense-Webster, USA) was introduced into the RA and the enlarged CS through the right femoral vein for 3-dimensional nonfluoroscopic, electroanatomical mapping (CARTO, Biosense-Webstar). The His bundle electrogram could not be identified around the usual area probably because the enlarged CS might have displaced the compact AV node and the proximal portion of the His bundle. The tachycardia was easily induced by either mechanical catheter contact or provocative

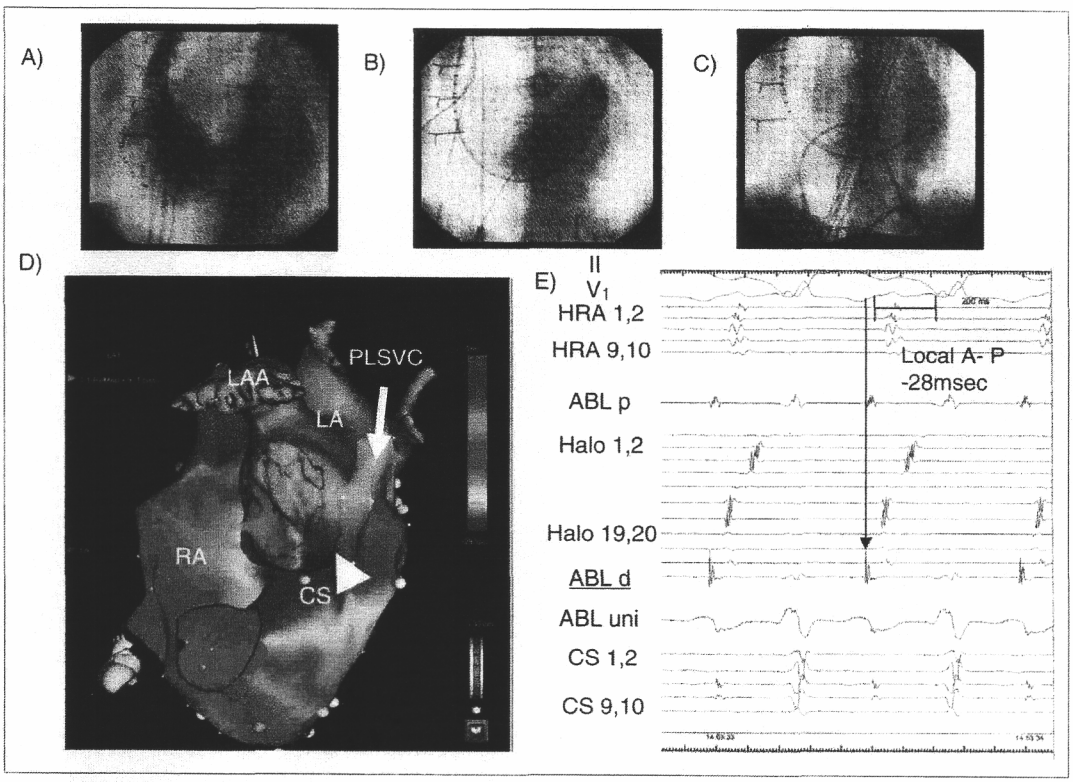

Figure 2

A) Right atrial angiogram (left anterior oblique view) **B**) Persistent left superior vena cava was visualized by contrast infusion into the distal CS. **C**) Position of the ablation catheter at the earliest activation site in the enlarged CS. **D**) Activation map during the tachycardia in the CARTO image merged with the multi-detector CT image (Left anterior oblique view). Arrowhead represents the earliest activation site. **E**) Surface electrocardiogram and intra-cardiac electrograms during the tachycardia. The vertical arrow indicates the origin of the P-wave on the surface electrocardiogram. Local A-P defines the time interval between the electrogram at the earliest site and the origin of the P-wave.

HRA: high in the RA. CS: coronary sinus, Halo: the tricuspid annulus, ABLd: the distal pair of electrodes of the ablation catheter, ABLp: proximal pair of electrodes of the ablation catheter

atrial pacing. Once it was induced, it incessantly terminated and reinitiated. The cycle length of the tachycardia varied from 420 ms to 500 ms with 1:1 or occasionally 2:1 AV conduction. Therefore, the conduction property of the anterograde/retrograde AV nodal pathways and the relation between the tachycardia origin and the location of the AV node could not be fully clarified. Intra-cardiac ECGs during the tachycardia showed an early atrial activation sequence in the mid CS despite changes in the cycle length. Within the distal to mid CS, multi-component electrograms were recorded. The earliest endocardial activation site was located at the top of the probable junction between the PLSVC and the CS, which was about 4.0 cm distal to the CS ostium (**Figure 2C**). The local electrograms preceded the onset of the P-wave by 28 ms and had a very sharp deflection as initial component (**Figure 2E**). The CARTO mapping in both the PLSVC/enlarged CS area and the RA demonstrated that the tachycardia propagated from the probable junction between the PLSVC and the CS into the RA in a centrifugal pattern (**Figure 2D**). The tachycardia was therefore diagnosed as an atrial tachycardia originating from the PLSVC/CS area due to local triggered activity or micro re-entry. Although RF energy (up to 20 W) was applied 3 times to the earliest site in a temperature controlled mode (maximum temperature: 50 °C), there were few remarkable changes in the atrial activation sequence of the tachycardia. We speculated that the tachycardia might originate from the epicardial site of the left atrium (LA) and that the RF energy might not be high enough to affect the tachycardia foci. However, we were concerned that the application of more frequent or higher RF energy delivery could cause vascular damage. Therefore, the RF energy was applied from the endocardial site of the LA, which allowed us to increase the frequency and quantity of energy delivered to the tachycardia foci. The CARTO map of the LA was

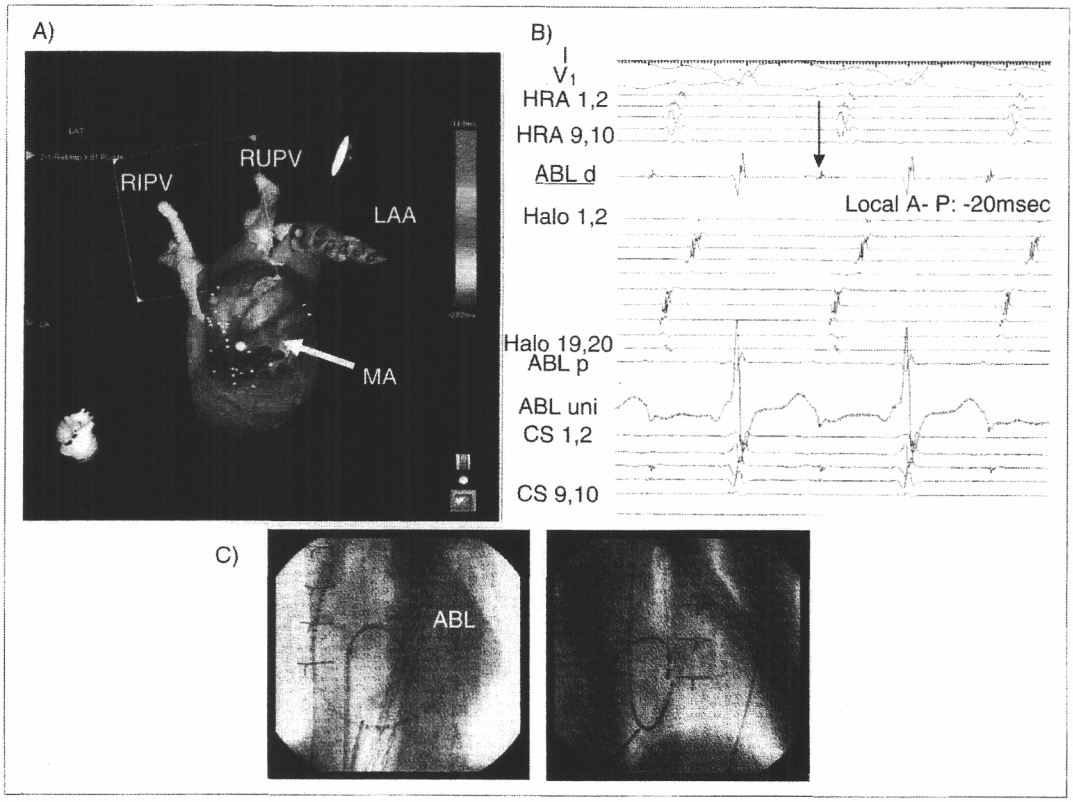

Figure 3

A) Inner view of the activation map during tachycardia in the CARTO image merged with the multi-detector CT image. Red tags represent RF application sites. The white tag shows the final RF application point. **B**) Surface electrocardiogram and intra-cardiac electrograms during the tachycardia. The vertical arrow indicates the origin of the P-wave. Local A-P defines the time interval between electrogram at the earliest site and the origin of the P-wave. **C**) The position of the ablation catheter at the earliest activation site in the endocardial LA (Left: left anterior oblique view. Right: right anterior oblique view)

merged with a multi-detector CT image before the ablation procedure. The merged image demonstrated that the tachycardia spread from the posteroseptal perimitral area, which was opposite to the earliest site in the CS over the LA wall (**Figure 3A**). The atrial electrogram at the earliest site in the LA preceded the onset of the P-wave by 20 ms (**Figures 3B** and **3C**). The RF energy was applied to the earliest site in the LA at a maximum power of 35 W to achieve 55 °C. **Figure 4** demonstrates intracardiac electrograms during termination of the tachycardia. The final application of RF energy gradually slowed and eventually terminated the tachycardia. After the termination, the AV interval remarkably prolonged to 380 ms in the sinus rhythm. A Wenckebach pattern of AV block appeared at a pacing cycle length of 500 ms. During RV apical pacing, VA conduction was very poor and observed only in the presence of isoproterenol. Tachycardia was no longer inducible even during intravenous infusion of isoproterenol. These findings strongly suggested that the application of RF energy to the posteroseptal perimitral area injured the antegrade/retrograde AV nodal pathways, thereby eliminating the substrate for the tachycardia circuit. On the basis of these data, we concluded that the tachycardia mechanism was not atrial reentry but fast/slow type AV nodal reentry.

After 6 months of follow-up, the patient was free of tachycardias. There was no advent of complete AV block. The echocardiography revealed improvement in the LVEF (51%).

Discussion

In the embryonic heart, pacemaker cells are available near both sinus horn and common cardinal vein sites. During the development of the heart, the left site transforms to a series of developmental remnants, the Marshall vein/ligaments and the CS.[1] These developmental remnants are reported to be associated with atrial arrhythmogenesis[3–8] since

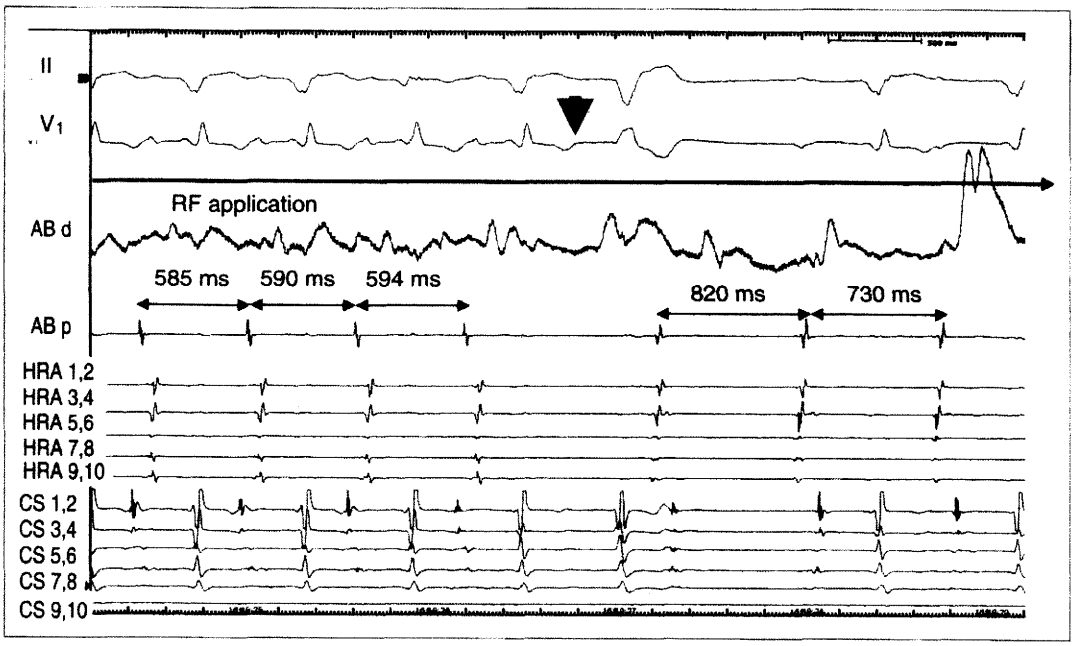

Figure 4 Long chart during RF application at the earliest site of the endocardial left atrium.
The horizontal arrow indicates the duration of RF application. The vertical arrowhead shows the termination of the tachycardia 15 seconds after start of RF application.

they retain their pacemaker function and ectopic automaticity. Especially in cases with PLSVC, more blood from the PLSVC could persistently stretch the CS wall and hence might cause increased arrhythmogenesis in the CS musculature.

Because of the irregularity in its cycle length and the occurrence of an incessant pattern, we first considered the tachycardia to be an atrial tachycardia that originated from the enlarged CS.[10] Badhwar et al. elegantly described the electrophysiological features of the atrial tachycardia in the boundary area between the CS and the LA and the outcome after RF ablation.[3] In most cases, the atrial tachycardia was successfully terminated by applying RF energy to the CS under guidance of a CS potential, which was characteristic of a discrete, sharp deflection and preceded the onset of the P-wave of the tachycardia. Application of RF energy to the endocardial site of the LA was not required.[3] Likewise in our case, a very sharp potential was recorded in multi-component electrograms at the earliest site of the CS; however, application of RF energy at this site hardly affected the tachycardia. Eventually, the tachycardia was terminated by application of RF energy to the earliest site of the LA opposite to the earliest site of the CS. Recordings during the final RF application (**Figure 4**) revealed that the tachycardia was terminated (disappearance of the P-wave) after the 5th beat. This finding implies that application of RF energy might either eliminate the tachycardia foci or block the retrograde pathways within the reentry circuit. Immediately after termination, neither ventricular premature beat nor the first sinus beat was conducted through the AV node. The subsequent sinus beats passed through the AV node with prolonged AV interval. Although VA conduction was observed only in the presence of isoproterenol, tachycardia was no longer inducible. Theses findings strongly suggest that the anterograde/retrograde AV nodal pathways were likely to form the tachycardia circuit. Since the tachycardia sustained even in the presence of an AV block before application of RF energy, the tachycardia was finally diagnosed as a fast/slow type AVNRT with lower common pathway.

Okishige et al. reported AVNRT cases in patients with PLSVC.[9] the enlarged CS due to the PLSVC might displace the compact AV node. They explained that during application of RF energy around the CS in patients with PLSVC much attention should be paid to avoid the occurrence of AV node injury and perforation of the CS.[9] It has been suggested that application of RF energy to the left anteroseptal or midseptal accessory pathways has a moderate risk to damage the compact AV node.[11] In our case, there was also a possible risk that the application of relatively high RF energy to the posteroseptal perimitral area could injure the AV

node, because the pathways and/or the compact AV node itself might be displaced; however, application to the CS did not affect the pathways. Before the final application of RF energy, it was difficult for us to differentiate a fast/slow AVNRT from an atrial tachycardia due to lack of information on the relationship between the tachycardia origin and the AV node.[10] Recently it has been suggested that the CS musculature is not only a source of atrial anrrhythmogenesis, but also may work as pathways for the interatrial conduction system in sinus rhythm or arrhythmias. Especially in AVNRT cases the CS musculatures are potentially involved in the reentrant circuit.[11,12] Therefore, we should have considered an uncommon type of AVNRT as the mechanism of the tachycardia, and have made a greater effort to identify the precise position of the AV node before RF energy application to confirm the mechanism of the tachycardia, and to avoid injury of the AV node.

Finally, in regard to the application of RF energy, the new 3-dimensional mapping system CARTO aided us in our case of a complex PLSVC/CS anatomy.

References

1) Morgan DR, Hanratty CG, Dixon LJ, et al: Anomalies of cardiac venous drainage associated with abnormalities of cardiac conduction system. Europace 2002; 4: 281–287
2) Singh B, Ramsaroop L, Maharaj J, et al: Case of double superior vena cava. Clin Anat 2005; 18: 366–369
3) Badhwar N, Jonathan M, Paul B, et al: Atrial Tachycardia Arising From Coronary Sinus Musculature. J Am Coll Cardiol 2005; 46: 1921–1930
4) Dave T, Angela C, Hwang C, et al: The ligament of Marshall. J Am Coll Cardiol 2000; 36: 1324–1327
5) Chauvin M, Shah D, Haissaguerre M, et al: The anatomic basis of connections between the coronary sinus musculature and the left atrium in humans. Circulation 2000; 101: 647–652
6) Tritto M, Zardini M, De Ponti R, et al: Iterative atrial tachycardia originating from the coronary sinis masculature. J Cardiovasc Electrophysiol 2001; 12: 1187–1189
7) Hsu LF, Jais P, Keane D, et al: Atrial Fibrillation originating from persistent left superior vena cava. Circulation 2004; 109: 828–832
8) Pavin D, Boulmier D, Daubert JC, et al: Permanent left atrial tachycardia: radiofrequency catheter ablation through the coronary sinus. J Cardiovasc Electrophysiol 2002; 13: 395–398
9) Okishige K, Fisher JD, Goseki Y, Azegami K, et al: Radiofrequency catheter ablation for AV nodal reentrant tachycardia associated with persistent left superior vena cava. Pacing Clin Electrophysiol 1997; 20: 2213–2218.
10) Knight BP, Ebinger M, Oral H, et al: Diagnostic value of tachycardia features and pacing maneuvers during supraventricular tachycardia. J Am Coll Cardiol 2000; 36: 574–582.
11) Nakagawa H, Jackman WM: Catheter ablation of paroxysmal supraventricular tachycardia. Circulation 2007; 116: 2465–2478
12) Nam GB, Rhee KY, Kim J, et al: Left atrionodal connections in typical and atypical atrioventricular nodal reentrant tachycaridas. J Cardiovasc Electrophysiol 2006; 17, 171–177.

Case Reports

Alternative Approach for Aortic Valve Replacement

in Mediastinal Deviation after Right Lobectomy

Kyokun Uehara, MD
Koji Ueyama, MD, PhD
Hidehiro Ito, MD
Kenichi Sasaki, MD
Ryuji Nohara, MD, PhD

A 71-year-old man on hemodialysis and with a history of right lobectomy was referred for aortic valve replacement. Chest computed tomography revealed counterclockwise rotation of the heart through its longitudinal axis.

We approached the aortic valve through median sternotomy. Accordingly, we transected the sternum at the level of the 3rd intercostal space and extended the skin incision approximately 2 inches perpendicular to the midline. After partial transection of the sternum, 3 spreaders were placed: the 1st, in the upper sternum; the 2nd, in the lower sternum; and the 3rd, between the ribs. These devices yielded excellent exposure of the ascending aorta. In addition, the relatively central shift of the ascending aorta contributed to the exposure of the right atrium and the right upper pulmonary vein. Subsequently, aortic valve replacement was performed in the usual fashion, and the patient experienced no postoperative respiratory complications. Aortic valve surgery with T-shaped sternotomy and without thoracotomy is an alternative technique in a patient who has a secondary deviation after lobectomy. ***(Tex Heart Inst J 2010;37(4):455-6)***

Although aortic valve replacement (AVR) is a well-known surgical procedure, AVR in a patient with secondary displacement has rarely been reported. Herein, we present an alternative surgical approach for surgery in the case of a patient with mediastinal deviation.

Case Report

In March 2009, a 71-year-old man on hemodialysis presented with chest pain and ST changes during electrocardiography after colectomy. Echocardiographic investigation revealed severe aortic valve stenosis (pressure gradient, 100 mmHg). The patient had undergone a right upper lobectomy for lung carcinoma 3 years earlier. The lobectomy had been performed through a right thoracotomy. Chest computed tomography revealed counterclockwise rotation of the heart through its longitudinal axis, with left pleural effusion (Fig. 1). Although right thoracotomy seemed to be a good approach for the displaced heart, adhesion in the right thoracic cavity was predicted. The patient's pulmonary function was poor because of chronic obstructive pulmonary disease. In order to protect the right lung, we decided to perform AVR through a complete median sternotomy.

After the pericardium was opened, only the main pulmonary artery and right ventricle were revealed. The ascending aorta and right atrial appendage were not visible. Accordingly, we transected the sternum at the level of the 3rd intercostal space and extended the skin incision approximately 2 inches perpendicular to the midline. The right internal thoracic artery was ligated and divided, and care was taken not to incise the pleura. After partial transection of the sternum, 3 spreaders were placed. The 1st spreader was placed in the upper sternum; the 2nd, in the lower sternum; and the 3rd, between the ribs. The use of these devices enabled excellent exposure of the ascending aorta. In addition, the relatively central shift of the ascending aorta contributed to the exposure of the right atrium and the right upper pulmonary vein.

Cardiopulmonary bypass was established via the ascending aorta with venous drainage through a 2-stage cannula in the right atrial appendage. After a cannula was inserted from the right atrium into the coronary sinus for retrograde cardioplegia, a vent tube was placed through the right upper pulmonary vein into the left ventricle in standard fashion. The ascending aorta was clamped, and retrograde cold-blood cardioplegic solution was delivered. A transverse aortotomy was performed at the level of the

Key words: *Aortic valve/surgery; cardiac surgical procedures; heart valve prosthesis implantation/methods; risk factors; treatment outcome*

From: *Department of Cardiovascular Surgery & Cardiology, Kitano Hospital, Osaka 530-8480, Japan*

Address for reprints: *Koji Ueyama, MD, PhD, Department of Cardiovascular Surgery, Kitano Hospital, 2-4-20 Ogimachi, Kita-ku, Osaka City, Osaka 530-8480, Japan*

E-mail: *k-ueyama@kitano-hp.or.jp*

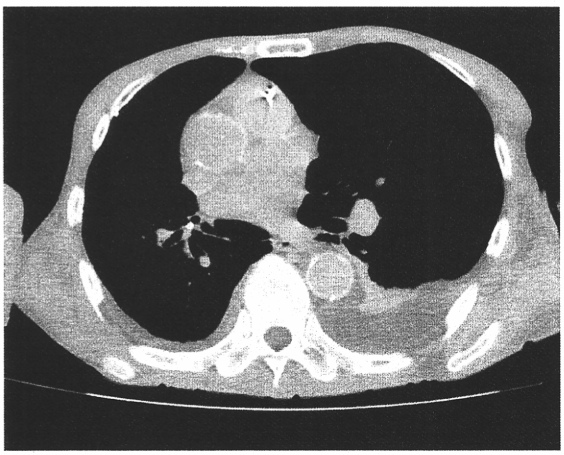

Fig. 1 *Computed tomogram shows displacement of the great arteries into the right chest. Left pleural effusion is present.*

sinotubular junction. Subsequently, the severely calcified native aortic valve was excised and replaced with a 19-mm Carpentier-Edwards bioprosthetic valve (Edwards Lifesciences LLC; Irvine, Calif). The patient's postoperative recovery was uneventful, with no respiratory complications. He remains under observation as an outpatient.

Discussion

Several approaches to aortic valve surgery have been used, including median sternotomy, right or left thoracotomy, and various minimally invasive approaches; however, the most common is median sternotomy.[1-5] The procedures other than median sternotomy have been used for reoperation for cosmetic reasons, or when the patient had patent internal thoracic artery grafts or mediastinal displacement.[1,2,5]

A thoracotomy approach to valve surgery involves technical difficulties. Svensson and colleagues[3] found a higher incidence of stroke in cases of right thoracotomy than in those of median sternotomy. They underlined the importance of the cannulation approach in order to reduce the risk of embolic stroke. Our patient had undergone dialysis for 20 years. Computed tomography showed severe calcification and arteriosclerosis in the descending aorta and femoral artery. In previous patients who also had arteriosclerosis, we used axillary artery cannulation. This was not possible in our patient, who had a dialysis shunt on his arm. Moreover, the adhesion between the 3rd and 4th intercostal spaces added to the difficulty of performing a right thoracotomy or using the right parasternal approach.

Several authors have reported AVR through left thoracotomy.[2,4] Barreda and colleagues[4] described this approach to valve surgery for the treatment of mediastinal displacement after pneumonectomy. Their patient had experienced a severe shift of the mediastinum into the left lung; hence, they could perform aortic valve surgery through a left thoracotomy. In our patient, left thoracotomy was undesirable because of the counterclockwise rotation of the mediastinum through its longitudinal axis.

In order to avoid embolic stroke and lung injury in our patient, we planned to expose the aortic valve through a median sternotomy; however, in order to achieve exposure, the sternum at the 3rd intercostal space had to be partially transected. Then, the 3 spreaders yielded excellent exposure of the ascending aorta and valve. In addition, the relatively central shift of the ascending aorta contributed to the exposure of the right atrium and the right upper pulmonary vein. The surgery was straightforward, and the patient experienced no postoperative respiratory dysfunction or other sequelae.

We conclude that aortic valve surgery with T-shaped sternotomy and without thoracotomy is an alternative technique in a patient who has a secondary deviation after lobectomy.

References

1. Rao PN, Kumar AS. Aortic valve replacement through right thoracotomy. Tex Heart Inst J 1993;20(4):307-8.
2. Hirose H, Umeda S, Mori Y, Murakawa S, Azuma K, Hashimoto T. Another approach for aortic valve replacement through left thoracotomy. Ann Thorac Surg 1994;58(3):884-6.
3. Svensson LG, Gillinov AM, Blackstone EH, Houghtaling PL, Kim KH, Pettersson GB, et al. Does right thoracotomy increase the risk of mitral valve reoperation? J Thorac Cardiovasc Surg 2007;134(3):677-82.
4. Barreda T, Laali M, Dorent R, Acar C. Left thoracotomy for aortic and mitral valve surgery in a case of mediastinal displacement due to pneumonectomy. J Heart Valve Dis 2008; 17(2):239-42.
5. Byrne JG, Karavas AN, Adams DH, Aklog L, Aranki SF, Filsoufi F, Cohn LH. The preferred approach for mitral valve surgery after CABG: right thoracotomy, hypothermia and avoidance of LIMA-LAD graft. J Heart Valve Dis 2001;10 (5):584-90.

Original Article

Voluntary Exercise Ameliorates the Progression of Atherosclerotic Lesion Formation via Anti-Inflammatory Effects in Apolipoprotein E-Deficient Mice

Kosuke Fukao[1], Kazunori Shimada[1], Hisashi Naito[2], Katsuhiko Sumiyoshi[1], Nao Inoue[3], Takafumi Iesaki[4], Atsumi Kume[1], Takashi Kiyanagi[1], Makoto Hiki[1], Kuniaki Hirose[1], Rie Matsumori[1], Hiromichi Ohsaka[1], Yasue Takahashi[1], Saori Toyoda[1], Seigo Itoh[1], Tetsuro Miyazaki[1], Norihiro Tada[5], and Hiroyuki Daida[1]

[1]Department of Cardiovascular Medicine, Juntendo University School of Medicine, Tokyo, Japan
[2]Department of Sports Science, Juntendo University Graduate School of Health and Sports Science, Chiba, Japan
[3]Laboratory of Food and Biomolecular Science, Graduate School of Agricultural Science, Tohoku University, Sendai, Japan
[4]Department of Organ and Cell Physiology, Juntendo University School of Medicine, Tokyo, Japan
[5]Atopy Research Center, Juntendo University Graduate School of Medicine, Tokyo, Japan

Aim: **A sedentary lifestyle with insufficient exercise is associated with cardiovascular disease. Previous studies have demonstrated that endurance exercise benefits atherosclerosis and cardiovascular disorders; however, the mechanisms by which physical activity, such as voluntary exercise (Ex), produces these effects are not fully understood.**

Methods and Results: **Eight-week-old male apolipoprotein (ApoE)-deficient mice were fed a standard diet (STD) or high fat diet (HFD) for 10 weeks. The HFD + Ex group mice performed Ex on a running wheel for 10 weeks. No significant differences in lipid profiles were observed between the HFD and HFD + Ex groups. Although changes in body and brown adipose tissue weights were comparable between the HFD and HFD + Ex groups, white adipose tissue weight was significantly lower in the HFD + Ex group than in the HFD group. The areas of atherosclerotic lesions in the aortic sinus and thoracoabdominal aorta were significantly reduced in the HFD + Ex group than in the HFD group ($p<0.001$). There was a strong negative correlation between atherosclerotic areas and the mean running distance per day in the HFD + Ex group ($r=-0.90$, $p=0.01$). Endothelial function was significantly preserved in the HFD + Ex group ($p<0.05$). Serum interleukin-6 and macrophage chemoattractant protein-1 levels were significantly lower and those of adiponectin were significantly higher in the HFD + Ex group than in the HFD group ($p<0.05$).**

Conclusions: **These results suggest that Ex ameliorates the progression of endothelial dysfunction and atherosclerotic lesion formation through anti-inflammatory effects, despite continued consumption of HFD.**

J Atheroscler Thromb, 2010; 17:1226-1236.

Key words; Voluntary exercise, Atherosclerosis, Endothelial function, Apolipoprotein E-knockout mice, Adiponectin

Introduction

Regular physical activity reduces the morbidity and mortality associated with cardiovascular diseases[1-3]. Physical exercise not only improves traditional risk factors, such as obesity, hypertension, dyslipidemia and glucose intolerance, but also the inflammatory state, which is closely linked to cardiovascular disorders[4, 5]. However, despite the wealth of evidence derived from epidemiological observations, interventional trials, and experimental animal studies, the mechanisms by which physical activity benefits ath-

Address for correspondence: Kazunori Shimada, Department of Cardiovascular Medicine, Juntendo University School of Medicine, 2-1-1, Hongo, Bunkyo-ku, Tokyo 113-8421, Japan
E-mail: shimakaz@juntendo.ac.jp
Received: December 15, 2009
Accepted for publication: July 6, 2010

4788(F)

erogenesis are not fully understood.

Exercise assessment models in mice use either voluntary or forced activity. Forced activities, such as swimming and treadmill exercise, have the advantage that mice can be made to exercise at reproducible duration and distances; however, these methods are non-physiological and stressful[6, 7]. Both swimming and treadmill exercises are unpleasant for mice because of the shock bar to avoid discontinuity of running or the fear of drowning[6, 7]; therefore, such unpleasant exercises may lead to adverse stress[8, 9]. Furthermore, these exercises are mostly performed during the day, in contrast to the nocturnal activity of mice. These factors are confounding for assessing the underlying mechanisms by which innate exercise, including the maintenance of physical activity, has beneficial effects on cardiovascular diseases. In contrast, voluntary running exercise can be performed in a non-stressful environment without disruption of the normal diurnal rhythm.

The present study aimed to assess the effects of voluntary exercise (Ex) on the initiation and progression of atherosclerotic lesions in apolipoprotein E (ApoE)-deficient mice. In addition, we examined the endothelial function of thoracic aorta, circulating pro- and anti-inflammatory parameters, and changes in white and brown adipose tissue weights, which play important roles in systemic inflammation. We demonstrated a marked reduction in atherosclerotic lesions, with a strong negative correlation between atherosclerotic areas and the mean running distance per day in mice fed a high-fat diet (HFD) supplemented with Ex. Moreover, voluntary running exercise ameliorated the progression of endothelial dysfunction and atherosclerotic lesion formation via anti-inflammatory effects, including an increase in adiponectin concentration followed by a decrease in the weight of white adipose tissue without a decrease in that of brown adipose tissue, despite continued consumption of HFD.

Materials and Methods

Experimental Animals

The Animal Care and Use Committee of Juntendo University School of Medicine reviewed and approved all protocols described in this study. ApoE-deficient mice were obtained from Jackson Laboratories (West Grove, PA). Male mice were provided with the diet and water and were maintained on a 12-h light/dark cycle in the specific pathogen-free facility of Juntendo University. The investigation conformed to the Guide for the Care and Use of Laboratory Animals published by the US National Institutes of Health (NIH Publication No.85-23, revised 1996).

Study Protocol

Experimental mice were weaned at 4 weeks of age and provided a normal chow diet (0.09% cholesterol and 5.6% fat; Oriental Yeast Co., Tokyo, Japan) until 8 weeks of age, and then randomly assigned to 3 groups as follows: a standard diet (STD), HFD, and HFD and Ex (HFD + Ex) groups. The STD group was provided a normal chow diet for 10 weeks. The HFD and HFD + Ex groups were provided a HFD (normal chow diet containing an additional 0.15% cholesterol and 15% fat; Oriental Yeast Co., Tokyo, Japan) for 10 weeks. The HFD + Ex group mice were kept in individual cages supplied with a running wheel (14 cm in diameter) and equipped with a counter to record the daily running rotation for 10 weeks. Mice were euthanized and sacrificed at 18 weeks of age and tissue samples were harvested immediately.

Histological Analysis of Atherosclerotic Lesions

Atherosclerotic lesions at the aortic sinus were analyzed by histological staining as follows. The upper portion of the heart and proximal aorta were obtained at sacrifice, embedded in OCT compound, and stored at −80℃. Serial 5-μm thick aortic cryosections beginning at the aortic root were collected from 200-μm segments of the aortic sinus, stained with saturated Oil Red-O solution at room temperature for 30 min, and counterstained with hematoxylin. For each mice, lipid lesions at the aortic sinus assessed as positive by Oil Red O-staining were quantified for the comparison of atherosclerotic lesions[10]. The ascending and descending aortas were dissected, cleaned of peripheral fat under a dissecting microscope to expose the endothelial surface, and stained with Sudan IV solution (0.5% wt/vol.; Sigma Chemical, St Louis, MO, USA). Aortic images were digitized using a microscope (Olympus AX80; Olympus Optical, Tokyo) equipped with a high-resolution camera (Nikon D2X; Nikon, Tokyo). The proportion of aortic intima surface area occupied by red staining of atherosclerotic lesions was quantified by normalizing the area stained with Sudan IV to that of the entire aorta using an imaging system (KS400; Carl Zeiss Imaging Solutions GmbH, Germany).

Endothelium-Dependent Relaxation to Acetylcholine

After the mice were sacrificed under anesthesia, their descending thoracic aortas were excised, cleaned of connective tissue, and cut into transverse vascular rings (approximately 2 mm in length). The protocol was conducted in temperasture-controlled (37℃) and

an oxygenated Krebs bicarbonate buffer (pH 7.4) containing the following: 118 mM NaCl, 4.7 mM KCl, 1.5 mM $CaCl_2$, 25 mM $NaHCO_3$, 1.1 mM $MgSO_4$, 1.2 mM KH_2PO_4, and 5.6 mM glucose, as we described previously[10]. Optimal passive tension of 0.5 g was applied to the vascular rings throughout the experiment. The vascular rings were initially exposed to a high-K^+ Krebs bicarbonate buffer containing 30 mM KCl instead of NaCl to produce maximal force generation and to enhance the reproducibility of subsequent contractions. After washing and observing a steady-state level of contraction, the vessels were submaximally contracted with 1.0 μM phenylephrine. The vasodilator responses to the endothelium-dependent agonist acetylcholine, the endothelium-independent agonist, and NO donor sodium nitroprusside were studied to investigate endothelial function. Relaxation was expressed as the percent change in the steady-state level of contraction. R_{max} was determined from the maximum relaxation of the established tone and ED_{50} was calculated from log transformation of the relaxation data.

Quantification of Lipids

Serum was separated by centrifugation and stored at −80℃. Serum total cholesterol and triglyceride levels and as well as lipoprotein concentrations were analyzed by an online dual enzymatic method for simultaneously quantifying cholesterol and triglycerides by high-performance liquid chromatography at Skylight Biotech Inc. (Akita, Japan), as we described previously[10].

Real-Time PCR

Total RNA from mouse thoracoabdominal aortas was extracted using a RNeasy Mini Kit (Qiagen) and treated with RNase-free DNase according to the manufacturer's instructions. Then, 1 μg RNA was reverse transcribed to cDNA with a High Capacity cDNA Reverse Transcription kit (Applied Biosystems, Foster City, CA, USA). Real-time PCR (7500 Real-time PCR System, Applied Biosystems) was used to determine mRNA levels of CD68 (macrophage marker), CD4 (T-helper cell marker), and CD11c (dendritic cell marker). TaqMan® Gene Expression Assays for CD68 (Cat # Mm00839636_g1), CD4 (Cat # Mm 00442754_m1), CD11c (Cat # Mm00498690_g1), and β-actin (Cat # Mm01205647_g1) were purchased from Applied Biosystems.

Measurement of Serum Parameters

Serum interleukin (IL)-6 and tumor necrosis factor (TNF)-α levels were measured using the Cytometric Bead Array Mouse Soluble Protein Master Buffer Kit (BD Biosciences). Serum monocyte chemoattractant protein (MCP)-1 and adiponectin levels were measured using commercial mice ELISA kits (Otsuka Pharmaceutical, Tokyo, Japan; R&D Systems, Minneapolis, MN, USA, respectively).

Statistical Analysis

Continuous variables are presented as the mean ± SD with the exception of analysis of vascular ring relaxation as the mean ± SEM. Differences between groups were analyzed by unpaired t-tests. Differences among 3 groups were analyzed by one-way ANOVA followed by appropriate post hoc analysis with a Bonferroni correction for multiple comparisons. Differences with $p<0.05$ were considered significant.

Results

Body Composition and Lipid Profiles

Table 1 shows the body weights and lipid profiles in the STD, HFD, and HFD + Ex groups. Body weight in the HFD + Ex group was slightly but significantly lower than in the HFD group at 18 weeks of age (HFD + Ex: 28.6 ± 1.0 g, HFD: 31.1 ± 0.9 g, $p<0.05$); however, there were no significant differences in the percent change in body weight from 8 to 18 weeks of age among the 3 groups. The mean running distance per day in the HFD + Ex group was 15,145 ± 3,619 m/24 h. There were no significant differences in food consumption, heart rate, or blood pressure among the 3 groups (data not shown). There were no significant associations between body weight changes and the mean running distance per day or body weight changes and food consumption. HFD induced a marked increase in total cholesterol in the HFD and HFD + Ex groups (HFD: 1,023 ± 170 mg/dL, HFD + Ex: 974 ± 330 mg/dL, STD: 521 ± 84 mg/dL, HFD vs. STD, $p<0.05$, HFD + Ex vs. STD, $p<0.05$); however, there was no significant difference between the HFD and HFD + Ex groups. The very low-density lipoprotein cholesterol levels were significantly higher in the HFD and HFD + Ex groups than in the STD group (HFD: 653 ± 146 mg/dL, HFD + Ex: 586 ± 297 mg/dL, STD: 295 ± 74 mg/dL, HFD vs. STD, $p<0.05$, HFD + Ex vs. STD, $p<0.05$). The high-density lipoprotein cholesterol or triglyceride levels were not significantly different among the 3 groups.

Table 2 presents a comparison of epididymal, perirenal, omental, and brown adipose tissues from fat pads among the STD, HFD, and HFD + Ex groups. The values of each fat/body weight of epididymal (10.1 ± 1.2 g/g × 1,000 vs. 7.8 ± 1.2 g/g × 1,000, $p<0.05$),

Table 1. Body weights and lipid profiles

	STD (n=8)	HFD (n=8)	HFD+Ex (n=8)
Initial BW, g	24.1±1.0	24.5±2.8	23.1±0.9
Final BW, g	29.9±1.4	31.1±0.9	28.6±1.0#
BW changes, %	23.9±9.8	28.5±15.6	24.2±7.3
Total cholesterol, mg/dL	521±84	1023±170*	974±330*
VLDL-cholesterol, mg/dL	295±74	653±146*	586±297*
LDL-cholesterol, mg/dL	191±51	285±75*	251±74
HDL-cholesterol, mg/dL	29±14	36±9	32±21
Triglyceride, mg/dL	33±22	32±17	30±6

Data are expressed as the mean±SD.
STD: standard diet, HFD: high fat diet, Ex: voluntary exercise, BW: body weight, VLDL: very low-density lipoprotein, LDL: low-density lipoprotein, HDL: high-density lipoprotein.
*$p<0.05$ vs. STD, #$p<0.05$ vs. HFD.

Table 2. Comparison of epididymal, perirenal, omental, and brown adipose tissues from fat pads among the STD, HFD, and HFD+Ex groups

	STD (n=6)	HFD (n=6)	HFD+Ex (n=6)
Epididymal fat/BW, g/g ×1,000	7.8±1.2	10.1±1.2*	7.4±1.6#
Perirenal fat/BW, g/g ×1,000	1.8±0.3	2.4±0.4*	2.1±0.3
Omental fat/BW, g/g ×1,000	3.0±0.6	3.1±0.9	2.4±0.4
BAT/BW, g/g ×1,000	2.2±0.5	1.9±0.4	1.8±0.3
WAT/BW, g/g ×1,000	12.5±1.9	15.5±2.4*	11.9±2.2#

Data are expressed as the mean±SD.
STD: standard diet, HFD: high fat diet, Ex: voluntary exercise, BW: body weight, BAT: brown adipose tissue, WAT: white adipose tissue (epididymal fat+perirenal fat+omental fat).
*$p<0.05$ vs. STD, #$p<0.05$ vs. HFD.

perirenal (2.4±0.4 g/g×1,000 vs. 1.8±0.3 g/g×1,000, $p<0.05$), and total white adipose tissues (15.5±2.4 g/g×1,000 vs. 12.5±1.9 g/g×1,000, $p<0.05$) were significantly higher in the HFD group than in the STD group. The values of epididymal (7.4±1.6 g/g×1,000 vs. 10.1±1.2 g/g×1,000, $p<0.05$) and total white adipose tissues (11.9±2.2 g/g×1,000 vs. 15.5±2.4 g/g×1,000, $p<0.05$) were significantly lower in the HFD+Ex group than in the HFD group. There was no significant difference in the values pertaining to brown adipose tissue among the 3 groups.

Voluntary Running Exercise Reduces Aortic Atherosclerotic Lesions in ApoE-Deficient Mice

Fig. 1 and **2** show atherosclerotic lesion formation in the aortic sinus and thoracoabdominal aorta, respectively, in the STD, HFD, and HFD+Ex groups. HFD for 10 weeks significantly induced atherosclerotic lesions in the aortic sinus (**Fig. 1B**, HFD: 19.9±7.0%, STD: 8.2±5.9%, $p<0.005$) and thoracoabdominal aorta (**Fig. 2B**, HFD: 31.6±6.1%, STD: 22.6±4.7%, $p<0.005$) in the HFD group. Histomorphometric analysis revealed that voluntary running exercise for 10 weeks significantly decreased atherosclerotic lesion formation in the HFD+Ex group than in the HFD group (**Fig. 1B**, HFD: 19.9±7.0%, HFD+Ex: 7.2±4.9%, $p<0.0005$, **Fig. 2B**, HFD+Ex: 18.6±4.4%, HFD: 31.6±6.1%, $p<0.0001$). Interestingly, there was a strong negative correlation between atherosclerotic areas in the thoracoabdominal aorta and mean running distance per day in the HFD+Ex group ($r=-0.90$, $p=0.01$) (**Fig. 3**).

Voluntary Running Exercise Preserves HFD-Induced Endothelial Dysfunction in ApoE-Deficient Mice

Fig. 4 shows cumulative concentration curves for acetylcholine and sodium nitroprusside in the phenylephrine-contracted rings of thoracic aortas from STD, HFD, and HFD+Ex mice. In this experiment, we added a STD with Ex (STD+Ex) group to assess whether exercise itself could improve acetylcholine- and sodium nitroprusside-induced relaxation. Endo-

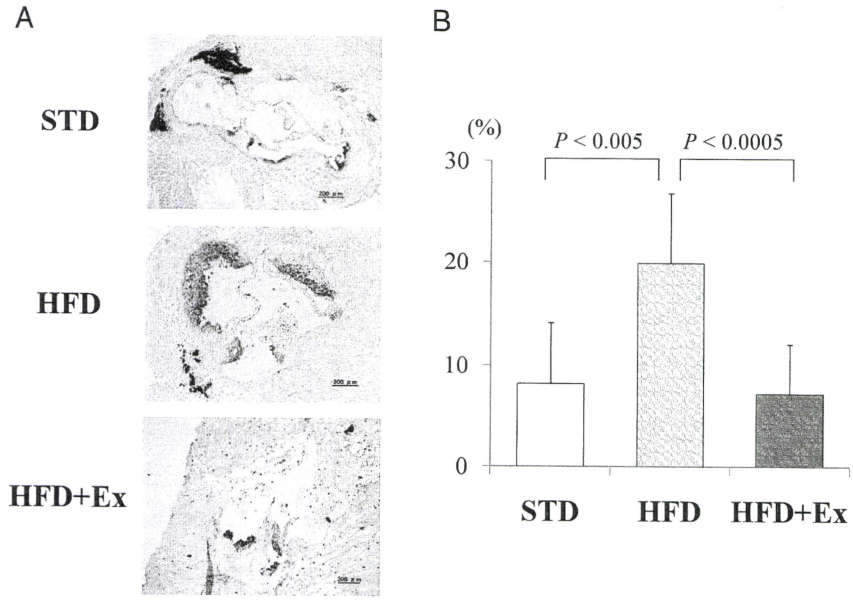

Fig. 1. Comparison of atherosclerotic lesion formation in the aortic sinus among the STD, HFD, and HFD + Ex groups.

Atherosclerotic lesion formation in the aortic sinus was determined by Oil red-O staining in the STD, HFD, and HFD + Ex groups. Representative examples (A) and histomorphometric analysis (B: mean ± SD; $n=6$ per group). The Y-axis is the percent area of atherosclerotic lesion formation in the aortic sinus.

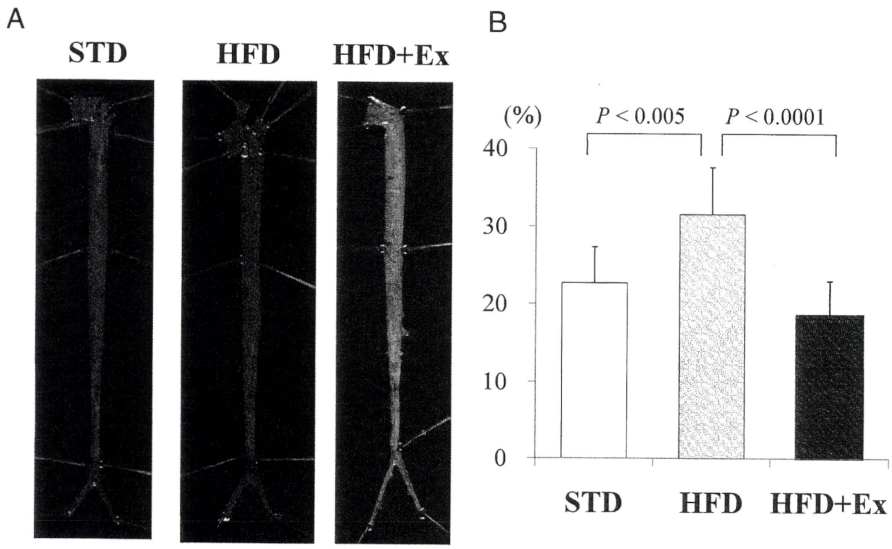

Fig. 2. Comparison of atherosclerotic lesion formation in the ascending and descending aortas among the STD, HFD, and HFD + Ex groups.

Ascending and descending aortas of STD, HFD, and HFD + Ex group mice were dissected to expose the endothelial surface, and developed for Sudan IV staining. Representative examples (A) and histomorphometric analysis (B: mean ± SD; $n=6$ per group). The Y-axis is the percent area of atherosclerotic lesion formation in the thoracoabdominal aorta.

thelium-dependent relaxation in response to acetylcholine at 1×10^{-8} (23.8±3.1% vs. 2.6±1.4%, $p<0.05$), 3×10^{-8} (50.5±3.3% vs. 12.6±3.0%, $p<0.05$), 1×10^{-7} (77.9±1.9% vs. 40.8±4.4%, $p<0.05$), 3×10^{-7} (92.4±0.9% vs. 66.5±3.4%, $p<0.05$), and 1×10^{-6} M (96.6±0.5% vs. 75.2±3.3%, $p<0.05$) was significantly higher in the HFD+Ex group than in the HFD group. The endothelium-dependent relaxation with acetylcholine at 1×10^{-8}, 3×10^{-8}, 1×10^{-7}, 3×10^{-7}, and 1×10^{-6} M was also significantly higher in the HFD+Ex group than in the STD group (all $p<0.05$). Endothelium-dependent relaxation with acetylcholine at 1×10^{-8} (17.5±2.8% vs. 2.6±1.4%, $p<0.05$), 3×10^{-8} (44.9±5.7% vs. 12.6±3.0%, $p<0.05$) 1×10^{-7} (75.7±4.0% vs. 40.8±4.4%, $p<0.05$), 3×10^{-7} (90.6±1.2% vs. 66.5±3.4%, $p<0.05$) and 1×10^{-6} M (96.0±0.7% vs. 75.2±3.3%, $p<0.05$) was significantly higher in the STD+Ex group than in the HFD group. Endothelium-dependent relaxation in response to acetylcholine at 1×10^{-8}, 1×10^{-7}, 3×10^{-7}, and 1×10^{-6} M was also significantly higher in the STD+Ex group than in the STD group (all $p<0.05$). In addition, endothelial-dependent relaxation with acetylcholine at 1×10^{-8}, 3×10^{-8}, 1×10^{-7}, 3×10^{-7}, and 1×10^{-6} M was significantly higher in

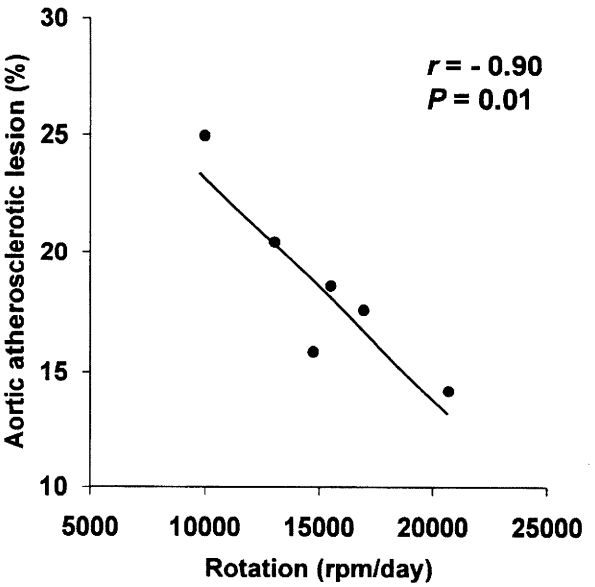

Fig. 3. Correlation between the percent area of atherosclerotic lesions in the thoracoabdominal aorta and the mean running distance per day.

Ascending and descending aortas from HFD+Ex group mice were dissected to expose the endothelial surface, and developed for Sudan IV staining ($n=6$).

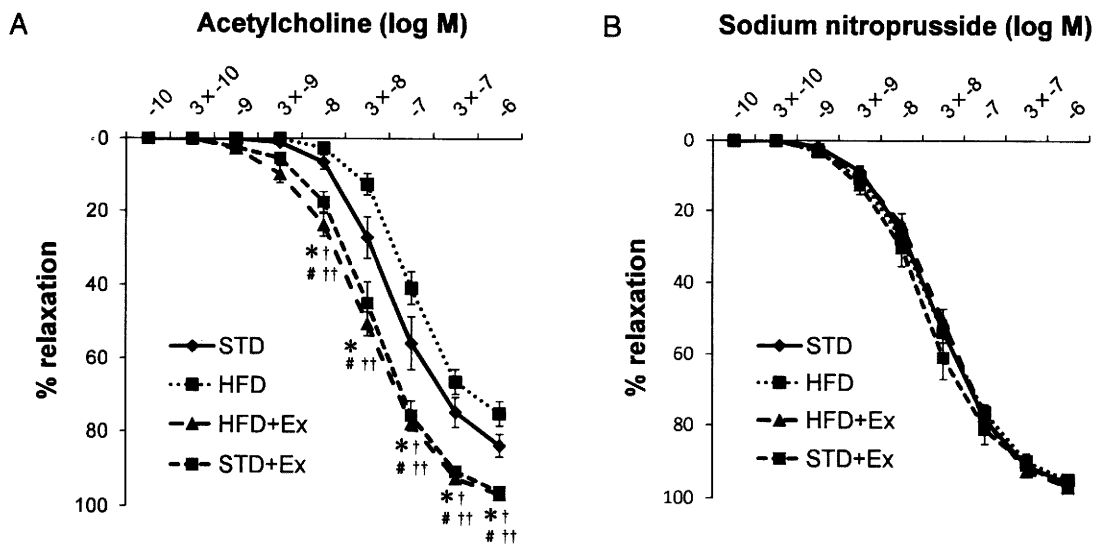

Fig. 4. Comparison of relaxation of vascular aortic rings with acetylcholine and sodium nitroprusside among the STD, HFD, HFD+Ex, and STD+Ex groups.

(A) Endothelium-dependent relaxation was elicited by the cumulative concentration of acetylcholine (0.1 nM-1 μM) in the STD ($n=12$), HFD ($n=12$), HFD+Ex ($n=11$), and STD+Ex ($n=12$) groups. (B) An endothelium-independent response was elicited by the cumulative concentration of sodium nitroprusside (0.1 nM-1 μM) in the STD ($n=12$), HFD ($n=12$), HFD+Ex ($n=11$), and STD+Ex ($n=12$) groups. The relaxation results are expressed as the percent change in the steady-state levels of 0.3 μM phenylephrine concentration. Error bars represent SEM. $^{*}p<0.05$ when compared between the HFD and HFD+Ex groups. $^{\#}p<0.05$ when compared between the STD and HFD+Ex groups. $^{\dagger}p<0.05$ when compared between the STD and STD+Ex groups. $^{\dagger\dagger}p<0.05$ when compared between the HFD and STD+Ex groups.

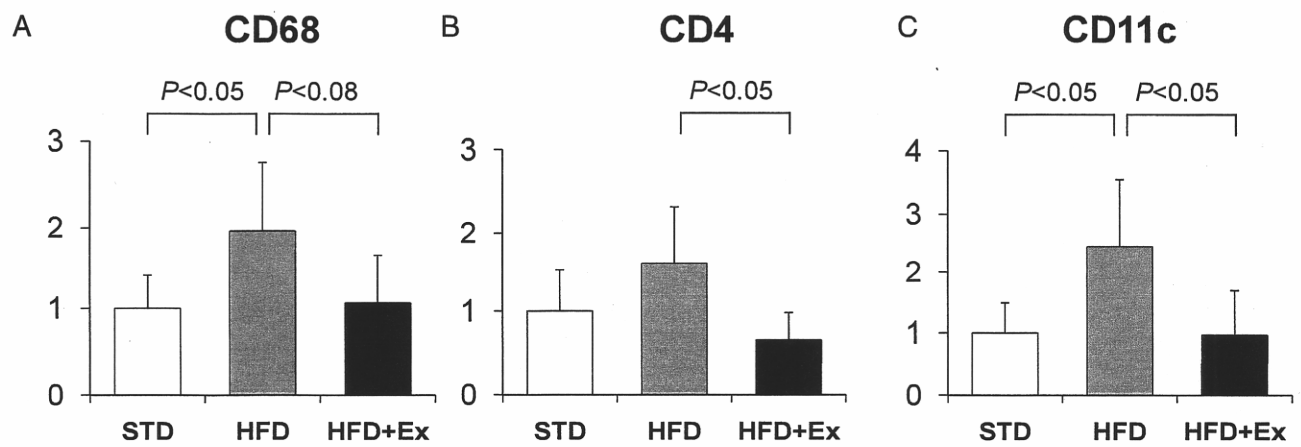

Fig. 5. Comparison of aortic mRNA expression for markers of inflammatory cells, i.e., macrophages, CD4 T cells, and dendritic cells among the STD, HFD, and HFD + Ex groups.

Levels of aortic mRNA expression of CD68, CD4, and CD11c were measured using real-time PCR in the STD (n=5), HFD (n=5), and HFD + Ex (n=5) groups at 18 weeks of age. Error bars represent SD.

the STD + Ex group than in the HFD group (all $p<0.05$). No significant differences were observed in endothelial-dependent relaxation between the STD + EX and HFD + Ex groups. Endothelium-independent relaxation in response to sodium nitroprusside was not different among the four groups.

Voluntary Running Exercise Decreases Aortic mRNA Expression for Markers of Inflammatory Cells

Fig. 5 shows the levels of aortic mRNA expression for markers of inflammatory cells, i.e., macrophages (CD68), CD4 T cells (CD4), and dendritic cells (CD11c). HFD significantly increased mRNA expression levels of CD68 (1.96 ± 0.78 vs. 1.00 ± 0.40, $p<0.05$) and CD11c (2.45 ± 1.11 vs. 1.00 ± 0.48, $p<0.05$) in the aortas of ApoE-deficient mice. The expression levels of CD4 (0.66 ± 0.32 vs. 1.60 ± 0.73, $p<0.05$) and CD11c (0.97 ± 0.72 vs. 2.45 ± 1.11, $p<0.05$) were significantly lower, and those of CD68 (1.06 ± 0.60 vs. 1.96 ± 0.78, $p<0.08$) tended to be lower in the HFD + Ex group than in the HFD group.

Voluntary Running Exercise Decreases Circulating Proinflammatory Cytokine Levels and Increases those of the Anti-Inflammatory Cytokine Adiponectin

Fig. 6 shows the levels of circulating proinflammatory cytokines and the anti-inflammatory cytokine adiponectin. HFD increased circulating IL-6 (14.6 ± 11.2 pg/mL vs. 4.3 ± 3.3 pg/mL, $p<0.05$), TNF-α (4.6 ± 3.2 pg/mL vs. 1.7 ± 0.8 pg/mL, $p<0.05$), and MCP-1 levels (177.7 ± 75.9 pg/mL vs. 99.4 ± 29.5 pg/mL, $p<0.05$), in ApoE-deficient mice. The serum IL-6 (2.5 ± 1.2 pg/mL vs. 14.6 ± 11.2 pg/mL, $p<0.05$) and MCP-1 levels (68.4 ± 34.3 pg/mL vs. 177.7 ± 75.9 pg/mL, $p<0.01$) were significantly lower, and those of TNF-α tended to be lower (1.9 ± 1.0 pg/mL vs. 4.6 ± 3.2 pg/mL, $p=0.07$) in the HFD + Ex group than in the HFD group. Adiponectin levels increased significantly in the HFD + Ex group (17.2 ± 2.2 μg/mL) compared to the HFD (13.9 ± 2.2 μg/mL) and STD (14.0 ± 2.2 μg/mL) groups (both $p<0.05$).

Discussion

This is the first study demonstrating that voluntary running exercise preserved endothelial function and ameliorated the progression of atherosclerotic lesions in the aortic sinus and thoracoabdominal aorta with a strong negative correlation between atherosclerotic areas and the running distance per day in ApoE-deficient mice. Moreover, Ex decreased the white adipose tissue weight, including that of epididymal fat, without loss of brown adipose tissue, whereas adiponectin levels increased and those of pro-inflammatory mediators, MCP-1, IL-6, and TNF-α, decreased.

Previous studies have shown that exercise training, such as on a treadmill and swimming, reduced atherosclerotic lesion formation and neointimal growth after carotid injury in mice models[11-18]; however, such unpleasant exercise may be forced under stressful conditions with disruption of the normal diurnal rhythm[6-9]. In contrast, voluntary running exercise can be performed to assess the underlying mechanisms by which